Available online at www.sciencedirect.com
ScienceDirect
Earth and Planetary Science Letters 255 (2007) 373–389
EPSL
www.elsevier.com/locate/epsl

Recent volatile evolution in the magmatic system of Hekla volcano, Iceland

Séverine Moune [a,*], Olgeir Sigmarsson [a,b], Thorvaldur Thordarson [b,c], Pierre-J. Gauthier [a]

[a] *Laboratoire Magmas et Volcans, CNRS—Université Blaise Pascal, 5 rue Kessler, 63038 Clermont-Ferrand Cedex, France*
[b] *Institute of Earth Sciences, University of Iceland, 101 Reykjavik, Iceland*
[c] *School of GeoSciences, University of Edinburgh, Grant Institute, Edinburgh EH9 3JW, UK*

Received 13 April 2006; received in revised form 15 December 2006; accepted 22 December 2006
Available online 8 January 2007
Editor: C.P. Jaupart

Abstract

Estimates of the volatile budgets for volcanic eruptions are often based on volatile concentrations measured in melt inclusions (MIs) versus groundmass glass. Here, we present new measurements and estimates of pre-eruptive volatile concentrations in magma from the Hekla volcano in Iceland based on MIs in recent basalts and basaltic icelandites from the 2000 eruption.

The last eruption at Hekla occurred from 26 February to 8 March, 2000. It began with a short sub-Plinian phase followed by lava effusion that produced 0.17 km^3 of basaltic icelandite. Volatile (S, Cl, F and H_2O) and major element concentrations were measured in MIs trapped in olivine and plagioclase phenocrysts contained in the basaltic icelandite from the 2000 eruption and in basalt erupted in 1913 from a fissure adjacent to the Hekla volcano. Same elements were measured in the groundmass glass from the 2000 tephra. The observed compositional range of MIs from the basalt ($MgO \leq 7.73\%$) to the basaltic icelandite ($MgO \geq 2.51\%$) is readily explained by fractional crystallisation, allowing the prediction of the evolution of dissolved volatile concentrations within the magma plumbing system beneath Hekla.

The incompatible behaviour of the volatile elements controls their concentrations in MIs during the crystal fractionation, and consequently the highest concentrations are found in the most evolved basaltic icelandite MIs, with the notable exception of sulphur. Volatile concentrations in the basaltic MIs exhibit strong linear correlations with K_2O and this relationship can be used to estimate the theoretical "expected" volatile contents in the basaltic icelandite melt just prior to eruption. Such an approach avoids underestimation of the pre-eruptive volatile contents measured in MIs and improves constraints on the volatile mass release into the atmosphere. The difference of volatile contents between "expected" concentrations and those present in the groundmass, scaled to the mass of erupted magma, yields maximum atmospheric mass loading of 0.10 Mt HCl, 0.17 Mt HF and 3.77 Mt SO_2 during the 2000 Hekla eruption, whereas calculations using the measured values in the inclusions give a significant lower mass yields of 0.05 Mt HCl, 0.17 Mt HF and 0.6 Mt SO_2. These results are discussed and compared to the data derived from remote sensing and snow (proxy of the gas phase) measurements.

Keywords: Hekla volcano; melt inclusions; sulphur; fluorine; chlorine; pre-eruptive contents; volatile release

* Corresponding author. Present address: Institute für Mineralogie, Callinstrasse 3, 30167 Hannover, Germany.
E-mail address: s.moune@mineralogie.uni-hannover.de (S. Moune).

0012-821X/$ - see front matter © 2007 Elsevier B.V. All rights reserved.
doi:10.1016/j.epsl.2006.12.024

1. Introduction

Volatiles released by volcanic eruptions link the atmosphere and the magma at depth from which they exsolve. The principal magmatic volatiles are water, carbon dioxide, sulphur species and halogens (e.g. Cl, F), and considerable quantities of these are emitted into the atmosphere, during eruptions, influencing the global climate (e.g. [1–3]). For obvious reasons it is difficult to measure directly the volatile emissions during explosive eruptions and therefore such measurements are typically obtained by remote sensing techniques. However, volatile emissions can also be estimated by the so-called "petrological method", one of the most used techniques to study ancient eruptions. In this approach, it is assumed that the volatile concentration in melt inclusions (MIs) preserved inside phenocrysts represents that dissolved in the magma at depth, whereas the volatile concentration in the groundmass glass of quenched eruption products represents the residual volatile concentration of the melt after degassing upon eruption (e.g. [4–6]). The difference in volatile contents between MIs and groundmass, scaled to the mass of erupted magma, can then be used to estimate the amount of each volatile species degassed for a given eruption (e.g. [6–8]). This approach is, however, considered to provide a minimum estimate of the volatile mass released since possible contributions from non-erupted magma at depth are not taken into account. At several subduction-related volcanoes for instance, this method yields significantly lower estimates of sulphur emission compared to results obtained by remote sensing techniques. This discrepancy between the two techniques, often referred to as "excess S", is attributed to the degassing of non-erupted magma and/or the accumulation of an immiscible SO_2- bearing fluid phase in the magma at depth (e.g. [5,9–11]). However, no "excess S" is observed at the few hot spot volcanoes studied so far [5,12].

In Iceland, estimates of S and also Cl and F degassing for a few eruptions have been presented [2,8,13]. In this study, we address the degassing history and volatile budget of the magmatic system at Hekla volcano with special emphasis on its last eruption in February 2000. Hekla is one of the most active volcanoes in Europe and its historical volcanic activity, petrology, and geochemistry have been the subject of several studies (e.g. [14–18]). Nevertheless, little is known about the volatile content of Hekla's magmas and their degassing behaviour upon eruption [12]. However, studies on fluorine from Hekla eruptions have shown that they released significant quantities of F into the atmosphere causing fluorosis in grazing animals and pollution in nearby rivers [19–21]. Furthermore, passive carbon dioxide and monoxide outgassing at the end of 1947–48 Hekla eruption killed wild birds as well as grazing animals (sheep) in the immediate vicinity of the volcano (e.g. [14]).

Major elements and volatile (Cl, S, F and H_2O) contents were measured in MIs in phenocrysts of variable compositions and in the groundmass glass of a basalt erupted in 1913 and the 2000 basaltic icelandite. In this paper we present these results and discuss the evolution of dissolved volatiles in the magmatic system of Hekla. These new results, combined with data from snow samples that represent the volatile composition of the 2000 eruptive plume [22], provide new insights on the volatile budget of the 2000 eruption.

2. Geological setting

Hekla volcano (63.98°N, 19.70°W; 1490 m a.s.l.) is located in the southern part of Iceland at the intersection of the South Iceland Fracture Zone and the Eastern Volcanic Zone (Fig. 1). The Eastern Volcanic Zone (EVZ) includes the four most active volcanic systems in Iceland: the Veidivötn, Grímsvötn, Katla and Hekla systems (e.g. [23]). While the first three mainly produce basaltic magma, the Hekla system has produced a suite of basalt, basaltic andesite, andesite, dacite and rhyolite magmas that belong to the transitional alkalic series [24]. To avoid confusion with intermediate rocks of the calc-alkaline series, we use here the terms basaltic icelandite and icelandite to describe the iron-rich intermediate rock compositions of Hekla.

All historical eruptions of Hekla begin with an highly explosive sub-Plinian to Plinian phase that normally is followed by a longer-lasting phase of effusive activity [14]. The final lava of most eruptions has uniform composition of basaltic icelandite, with SiO_2 close to 54% [17,18,22]. Basalts never erupt from the Hekla center but are emitted through eruptive fissures in its close vicinity. The basaltic icelandites are most likely formed by 62–63% fractional crystallisation of plagioclase, olivine, clinopyroxene and titanomagnetite from a basaltic magma similar to the magma extruded in the surrounding fissure eruptions [18]. Geodetic measurements indicate the presence of a magma chamber at approximately 9 km depth beneath the volcano [25].

The 2000 Hekla eruption lasted for 12 days, from 26 February to 8 March. It began with a 2-hour-long sub-Plinian phase, with peak discharge during the first hour of activity when the eruptive column reached approximately 11 km [26]. As a whole, the 2000 eruption produced 0.17 km^3 of basaltic icelandite magma [26], of which $\approx$0.01 km^3 was deposited as tephra [23,27]. The

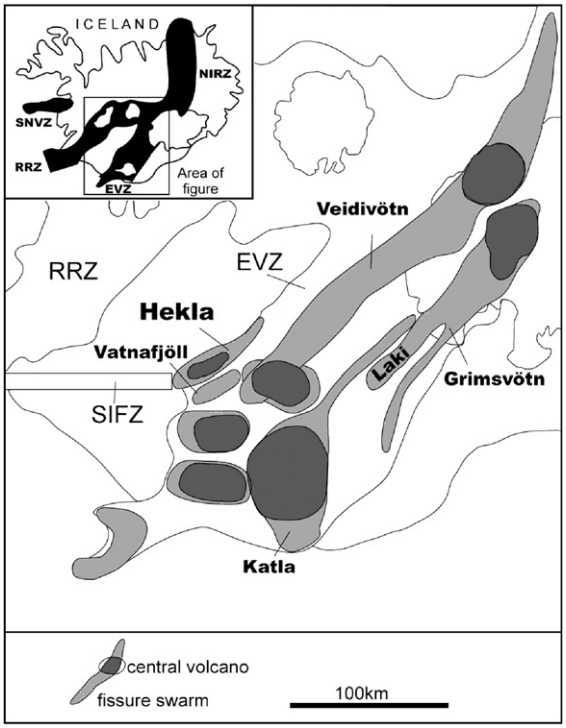

Fig. 1. Simplified map of the Eastern Volcanic Zone (EVZ) in Iceland (modified from [13,24]). The following volcanic systems are shown: Hekla, Vatnafjöll, Veidivötn, Grímsvötn and Katla. Hekla volcano is located at the junction of the South Iceland fracture zone (SIFZ) and the EVZ. Inset: The neovolcanic zones of Iceland (RRZ: Reykjanes Rift Zone, SNVZ: Snæfellsnes Volcanic Zone, NIRZ: North Icelandic Rift Zone).

gas phase and the eruption column were studied by satellite-based techniques [28], aircraft observations [29], ground-based radar measurements [26] and through the analysis of snow-condensed volatiles [22]. Degassing estimates based on analysis of a few MIs in the 2000 products of Hekla were found to be compatible with satellite-based gas-sensing measurements [12]. These first results are integrated with our new analyses for comparing volatile budgets derived from MI data and remote sensing measurements, respectively.

3. Sample description

We collected two tephra samples for this study labelled Hek-16T and HK2000T. The sample Hek-16T is lapilli scoria from one of the cones on the A.D. 1913 Lambafit fissure, which is the youngest basaltic eruption on Hekla volcanic system [14]. HK2000T is basaltic icelandite tephra from the first phase of the 2000 eruption, collected freshly fallen at a site located ≈18 km to the north of the volcano. Volcanic products from the Hekla system are poor in phenocrysts (around 5%; [24]), making the separation of crystals containing MIs a tedious process. Olivine and plagioclase phenocrysts were hand-picked under a binocular microscope from a 250–600 μm grain size fraction of crushed tephra. The crystals were mounted on a thin section for identification of minerals containing MIs. Then the MI-bearing phenocrysts were washed with acetone, embedded in epoxy and polished individually to produce adequate exposure of the MIs for microprobe measurements.

The MIs in olivine and plagioclase from Hek-16T are typically spherical to oblate (essentially in plagioclase) and with a size range of 10–150 μm. Shrinkage bubble are common in these MIs but they are totally deprived of daughter minerals (Table 1; see [4,30] for definitions). The olivine phenocrysts in the basaltic icelandite contain pristine but small (5–30 μm) MIs that occasionally feature a shrinkage bubble but no daughter minerals (Table 2). The plagioclase phenocrysts of the basaltic icelandite generally contain partially crystallised MIs and consequently are not included in this study.

The groundmass of the Hek-16T scoria grains is holocrystalline, whereas that of HK2000T tephra contains 25% microlites of plagioclase (21%) and pyroxene (4%), with only small patches of interstitial glass (<20 μm in diameter).

4. Analytical methods

4.1. Electron microprobe analysis

Major and volatile element compositions of host minerals, MIs and groundmass were measured on a SX-100 CAMECA electron microprobe (EMP) at LMV (Clermont-Ferrand) using 15 kV accelerating voltage. Sample currents and counting times used for analysing different groups of elements are listed in Table 3. A focused beam of 1 μm was used for minerals but in order to reduce Na loss, a 5 μm defocused beam was employed during glass analysis. Our MI analysis of the basalt does not appear to underestimate Na concentrations, whereas those for the basaltic icelandite exhibit significant Na-loss (Table 2). Several test runs on a silica-rich standard glass reveal that a defocused beam larger than 15 μm is required to prevent loss of Na during analysis (e.g. [31]). However, such an approach could not be applied here because of the small size of the MIs. It is possible to correct this Na-loss by monitor the count rate for Na and extrapolate time zero. Inherently, this approach leads to Na measurements with poor precision and therefore has not been adopted here. Consequently, Na concentrations in HK2000T inclusions are underestimated and will not be further discussed.

Analyses of Cl, S and F were performed with 80 nA sample current and 200 s acquisition time using LPET diffraction crystal (Cl and S) and 400 s on a TAP crystal (F; Table 3). In order to minimize volatile losses during analysis, the beam was blanked regularly with the Faraday cup and counts were collected in 20 s intervals by 10 iterations for Cl and S, and 20 iterations for F [8]. Variations in the wavelength of sulphur Kα X-ray as a function of its oxidation state [32,33] in silicate glasses were taken into account during S analysis. Error assessments and detection limits were calculated using the statistical methods developed for microanalyses by

Table 1
Melt inclusion (MI) and whole rock major and volatile compositions (in wt.%) in Hekla basalt (Hek-16T)

Samples	Whole rock	MIs in olivines in Hek-16T										MIs in plagioclases in Hek-16T				
	Hek-16T	FL	C	DL	EL	AL	A	2A	D	GL	Mean (±SD)	P3	P2	P1	P1-2	Mean (±SD)
SiO_2	45.4	48.1	46.8	47.6	47.1	46.4	46.9	46.7	47.5	45.6	47.0 (0.75)	46.3	46.2	45.6	45.7	46.0 (0.31)
TiO_2	4.66	2.36	2.69	2.73	3.04	3.06	3.23	3.18	4.18	4.68	3.24 (0.74)	4.37	4.56	4.68	4.47	4.52 (0.13)
Al_2O_3	13.3	15.3	14.5	14.9	14.0	14.3	14.5	14.2	14.4	12.9	14.3 (0.67)	13.0	12.9	12.6	13.0	12.9 (0.19)
FeO* [a]	15.9	9.23	10.4	12.2	12.8	13.2	12.2	12.3	12.5	15.4	12.2 (1.72)	14.4	14.8	14.6	14.7	14.6 (0.19)
MnO	0.29	0.15	0.17	0.20	0.20	0.21	0.19	0.19	0.21	0.26	0.20 (0.03)	0.24	0.25	0.25	0.25	0.25 (0.01)
MgO	4.48	6.78	7.73	6.84	6.97	6.72	6.30	6.45	4.60	5.07	6.38 (0.97)	5.27	5.32	5.28	5.12	5.25 (0.08)
CaO	9.56	13.6	11.6	11.3	11.0	10.7	11.3	11.1	10.9	9.35	11.2 (1.09)	9.03	9.00	9.25	9.11	9.09 (0.11)
Na_2O	2.68	2.31	2.49	2.61	2.67	2.62	2.81	2.65	2.96	2.83	2.66 (0.19)	2.85	2.79	2.80	3.02	2.86 (0.11)
P_2O_5	0.500	0.220	0.302	0.289	0.317	0.327	0.345	0.317	0.571	0.620	0.368 (0.13)	0.660	0.582	0.575	0.653	0.618 (0.05)
K_2O	0.620	0.341	0.427	0.361	0.440	0.473	0.459	0.441	0.628	0.643	0.468 (0.10)	0.704	0.671	0.693	0.677	0.686 (0.01)
Cl	–	0.012	0.017	0.016	0.017	0.019	0.019	0.019	0.026	0.025	0.019 (0.004)	0.020	0.025	0.024	0.025	0.024 (0.002)
S	–	0.144	0.154	0.144	0.167	0.157	0.160	0.151	0.218	0.263	0.173 (0.04)	0.206	0.258	0.252	0.233	0.237 (0.02)
F	–	0.023	0.031	0.037	0.040	0.038	0.044	0.038	0.067	0.065	0.043 (0.01)	0.043	0.063	0.052	0.044	0.050 (0.01)
H_2O	0.00 [b]	0.712	–	0.580	–	–	–	–	–	0.560	0.617 (0.08)	–	–	–	–	–
Sum	97.3	99.3	97.3	99.8	98.7	98.3	98.5	97.8	98.7	98.2	98.5	97.0	97.3	96.7	97.1	97.0
Fo [c]		84	84	80	78	78	78	78	74	71	78					
An [c]											–	66	66	66	66	66
Mg # [d]	37.7	61.2	61.6	54.5	53.9	52.2	52.7	52.9	44.1	41.5	52.7	44.1	43.6	43.7	42.8	43.5
X% [e]		2.4	5.5	4.7	5.9	5.1	7.6	8.7	0	0	4.4	0	0	0	0	0
Bubble		Yes	Yes	Yes	Yes	Yes	Yes	Yes	No	Yes		Yes	Yes	Yes	Yes	
Bubble size [f]		≈2%	≈3%	≤1%	≈3%	<1%	<1%	<1%		≈6%		≈2%	≈2%	≈2%	≤1%	

–: Not determined.
[a] Total iron as FeO.
[b] Loss on ignition (LOI) in wt.%.
[c] Fo (mol.%) and An (mol.%) represent the host mineral compositions.
[d] Mg # is the molecular ratio: [Mg/(Mg+Fe)]*100 of glass (Fe as Fe^{2+} only).
[e] *X* is the percentage of post-entrapment host olivine crystallisation on MI rims.
[f] Approximate size of bubble in the inclusion in vol.%, assuming spherical shape for MI and its bubble, determined from photographs.

Table 2
Melt inclusion (MI), groundmass and whole rock major and volatile compositions (in wt.%) in Hekla basaltic icelandite (HK2000T)

Samples	Whole rock [a]	MIs in olivine in HK2000T											Groundmass	Groundmass corrected
	HK2000T	3L	2L	1	1–2	2	3	4	5	5–2	5–3	Mean (±SD)	HK2000T (±SD)	HK2000T
SiO_2	54.6	54.3	52.4	54.6	54.2	54.2	54.3	54.0	53.8	54.1	56.5	54.3 (0.99)	55.2 (1.04)	–
TiO_2	2.16	2.03	1.96	2.03	2.01	2.02	2.07	2.04	2.05	2.05	2.12	2.04 (0.04)	2.09 (0.07)	–
Al_2O_3	14.4	13.8	13.2	14.0	13.9	14.0	14.0	14.0	13.8	14.1	14.2	13.9 (0.27)	14.1 (0.26)	–
FeO* [b]	11.6	11.3	13.8	11.5	11.5	11.6	11.5	11.8	11.6	11.7	12.2	11.9 (0.73)	11.5 (0.63)	–
MnO	0.37	0.29	0.32	0.29	0.29	0.29	0.27	0.30	0.29	0.28	0.30	0.29 (0.01)	0.29 (0.03)	–
MgO	2.50	2.60	3.32	2.75	2.81	2.70	2.76	2.51	2.54	2.62	2.55	2.72 (0.24)	2.97 (0.18)	–
CaO	6.61	6.50	6.59	6.54	6.47	6.61	6.41	6.79	6.79	6.98	7.19	6.69 (0.25)	6.48 (0.31)	–
Na_2O	4.10	2.783	3.034	2.362	3.003	2.991	3.304	2.762	2.623	2.563	0.195	2.56 (0.57)	3.16 (1.08)	–
K_2O	1.23	1.22	1.12	1.23	1.23	1.24	1.23	1.16	1.19	1.19	1.08	1.19 (0.05)	1.44 (0.10)	1.16
P_2O_5	1.10	1.01	1.08	1.03	0.99	1.01	1.04	1.02	1.07	1.09	1.08	1.04 (0.04)	1.06 (0.05)	–
Cl	–	0.039	0.040	0.040	0.039	0.038	0.038	0.040	0.041	0.039	0.042	0.040 (0.001)	0.037 (0.003)	0.028
S	–	0.092	0.094	0.092	0.094	0.091	0.086	0.094	0.097	0.092	0.099	0.093 (0.004)	0.027 (0.004)	0.020
F	–	0.121	0.120	0.132	0.098	0.111	0.110	0.127	0.132	0.123	0.139	0.121 (0.01)	0.111 (0.002)	0.084
H_2O	0.00 [c]	–	–	–	–	2.42	–	–	–	–	–	2.4	–	–
Sum	98.7	96.1	97.2	96.6	96.5	99.4	97.2	96.7	96.0	97.0	97.7	97.0	98.5	–
Fo [d]		58	58	58	58	58	58	58	58	58	58	58		
Mg # [e]	31.6	32.5	33.5	33.5	33.9	32.7	33.4	30.9	31.5	31.9	30.5	32.4	35.1	–
Bubble		Yes	Yes	No	No	No	No	Yes	No	No	No			
Bubble size [f]		≤1%	≤1%					≈ 5%						

–: Not determined.
[a] Data from [22].
[b] Total iron as FeO.
[c] Loss on ignition (LOI) in wt.%.
[d] Fo (mol.%) represents the host olivine compositions.
[e] Mg # is the molecular ratio: [Mg/(Mg+Fe)]*100 of glass (Fe as Fe^{2+}only).
[f] Approximate size of bubble in the inclusion in vol.%, assuming spherical shape for MI and its bubble, determined from photographs.

Ancey et al. [34]. The EMP precision (2σ), for a given element, was estimated from the propagated error in number of counts per second, at the signal peak and the background, for both the standard glass and the sample. This 2σ uncertainty is <5% for major elements, except for MnO, K_2O and P_2O_5 in the Hek-16T, and for MnO and P_2O_5 in HK2000T where it is <10%. The estimated 2σ precision for Cl, S and F is dependent on concentrations and is between 3–6%, 3% and 8–22%, respectively. Detection limits for S, Cl and F were 2, 20 and 200 ppm, respectively. Both reproducibility and accuracy of major and volatile (Cl, S and F) analyses were established by replicate analyses of glass standard (VG-A99 and Ke12) and are given in Table 4 with the published accepted values of these standards [8,35–37]. Two points were measured in most MIs and the average is given in Tables 1 and 2, except in the smallest inclusions where only one point could be measured.

4.2. Secondary ion mass spectrometry

The concentration of dissolved water in the largest melt inclusions (>30 μm) was determined by Cameca IMS 3f secondary ion mass spectrometry (SIMS) at CRPG (Nancy, France). The operating conditions used are as follows: a primary O^{2-} beam of 10 nA intensity, energy filtering of 10 eV, and a maximum spot size of 30 μm. Count rates were normalized to ^{30}Si, and a calibration curve was established between H_2O/SiO_2 in wt.% and $^1H/^{30}Si$ on basaltic glass standards

Table 3
Analytical conditions for EMP measurements

	Sample current (nA)	TAP [a]	PET [a]	PET [a]	LLIF [a]	LPET [a]
Minerals	15	$Na_{(10)}$ $Mg_{(20)}$ $Si_{(10)}$ $Al_{(20)}$	$K_{(30)}$	$Ca_{(30)}$	$Fe_{(20)}$ $Ni_{(30)}$ $Mn_{(20)}$	
Glasses	8	$Na_{(10)}$ $Si_{(10)}$ $Al_{(10)}$	$Ti_{(40)}$	$Ca_{(40)}$	$Fe_{(40)}$	
	30	$Mg_{(60)}$	$K_{(60)}$	$P_{(60)}$	$Mn_{(60)}$	
	80	$F_{(400)}$				$Cl_{(200)}$ $S_{(200)}$

Counting time in seconds is given in parenthesis.
[a] Abbreviations of diffraction crystal types.

Alv1833-11 and Wok28-3, which have 1.17 and 0.49 wt.% water contents, respectively [38]. Analytical precision on the water concentrations is 15% (2σ; [38]). Glass patches in the groundmass of HK2000T are too small ($\leq$20 μm) for analysis with this technique. Therefore, the loss on ignition (LOI) in wt.% in bulk samples is considered here as an approximation of the groundmass water contents. The major element concentrations of whole rock Hek-16T and HK2000T samples were measured by ICP-AES in Clermont-Ferrand and have a 2σ uncertainty between 5 and 10%.

4.3. Correction for late-stage crystallisation

In order to obtain the original liquid composition, the MI analysis must be corrected for host crystallisation on the MI rims after melt entrapment. For MIs in olivine, this correction uses the well established melt-olivine equilibrium constant, K_D $(=(FeO/MgO)_{ol}/(FeO/MgO)_{melt})$ between ferrous iron and magnesium [39]. However, the relative proportions of Fe_2O_3 and FeO in the melts considered in this study are unknown. Therefore, the Fe_2O_3/FeO^* of 0.17 obtained from whole-rock analyses of Hekla basalt [24] is taken here to be representative for MIs in the Hek-16T basalt. Applying this ratio and the model of Toplis [40] we obtain a K_D value of 0.31. This K_D value was used to compute, by dissolving numerically 0.1 wt.% increments of olivine into the melt, the equilibrium between different olivine compositions and the corresponding basaltic MI and thereby the amount of post-entrapment crystallisation (X), which ranges from 2% to 9% (Table 1). On the other hand, MI compositions in plagioclase from the basalt were not corrected because they fall on the magma evolution trend defined by the corrected olivine MI compositions (Fig. 2) and bulk Hekla lavas. Therefore, MIs in plagioclase can be considered to be in equilibrium with their host minerals and unaffected by post-entrapment crystallisation.

For MIs in olivines of the basaltic icelandite, the Fe_2O_3/FeO^* is calculated as 0.16 using the approach of Kilinc et al. [41] and the fO_2 and $T°$ values obtained by Baldridge et al. [15] for the 1970 basaltic icelandite of Hekla. Note that the products of the 1970 eruption are compositionally identical to that of the 2000 eruption. The fO_2 value used here is close to the FMQ-buffer, in agreement with estimates by Sharma et al. [12]. Using these values, the model of Toplis [40] gives a K_D of 0.32 for MIs in the basaltic icelandite, implying that the melt they represent is in equilibrium with their host olivines. Hence, correction for host-crystallisation is not required.

The Hekla 2000 groundmass typically contain significant amount of microlites formed by crystallisation upon cooling or degassing. Consequently, the concentrations of incompatible elements, such as S, Cl, F and K_2O, in the final groundmass liquid is increased proportionally to the amount of microlite crystallisation and therefore the measurements overestimate the concentrations of these elements in a microlite-free melt. Hence to obtain the concentrations of residual volatiles in pure (i.e. microlite-free) melt, we correct our groundmass measurements for this bias induced by microlite crystallisation. The amount of this late crystallisation stage was determined for the basaltic icelandite groundmass glass using a scanning electron microscope (SEM, JEOL 5910 LV) at Clermont-Ferrand. The back-scattered electron (BSE) imaging together with image analysis software were used to determinate the proportion of each groundmass phase (75 modal% glass, 21% plagioclase and 4% pyroxene). Concentrations of S, Cl and F, measured by the EMP, are below detection limit in all crystal phases and volatile concentrations measured in the groundmass glass were multiplied by 0.75 to obtain the microlite-free melt values. On the other hand, the plagioclase microlites contain 0.36 wt.% K_2O and therefore the measured K_2O values were corrected using the multiplication factor of 0.81. Corrected values are listed in Table 2 together with the measured values. Note that we have not applied this correction procedure to the other major elements.

5. Results

5.1. Phenocryst composition

The Hek-16T basalt is amongst the most primitive Holocene basalts around Hekla [18]. However, its low MgO concentration (4.5 wt.%; Table 1) illustrates the evolved character of transitional alkaline basalts in

Fig. 2. Major elements versus K_2O showing the compositional evolution of melt inclusions, basaltic icelandite groundmass, and whole rocks for the Hekla magmatic system. The major element raw analysed values for basaltic icelandite groundmass are plotted. The lava composition of the Vatnafjöll system, which is situated immediately east of Hekla, is indistinguishable from those of Hekla suggesting a common origin. Whole-rock data are from [18,22,24] and Sigmarsson (unpublished data). Analyses reported in [14,16] for the 1913 basalt (same eruption as our sample Hek-16T) fall on the evolutionary trends. Error bars of this study are given for MIs and groundmass at the 2σ confidence level. Sodium concentrations in the HK2000T inclusions were underestimated in this study and are not shown. Observed data scatter most likely is due to compilation of analyses from different laboratories using variable analytical techniques.

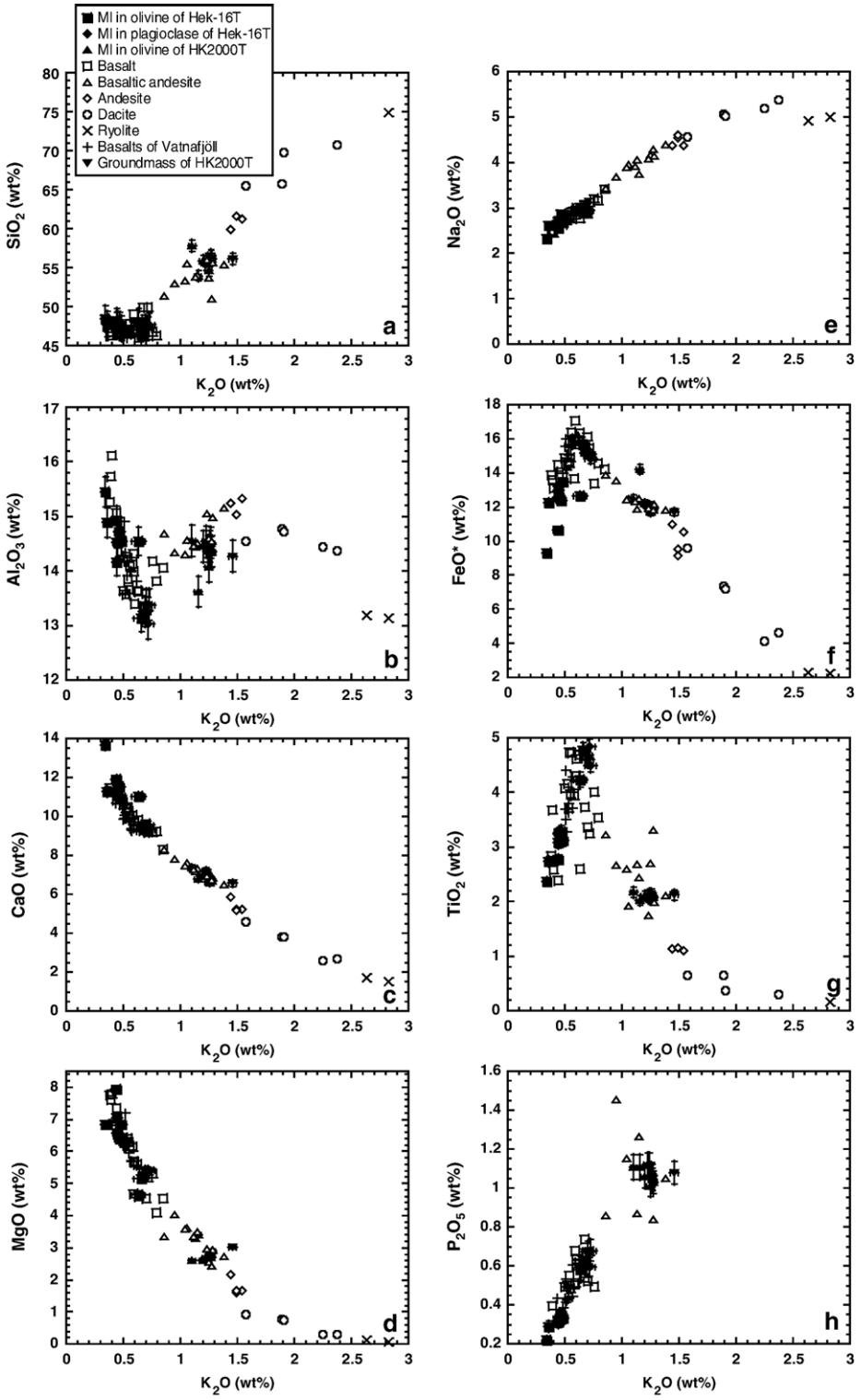
MI in olivine of Hek-16T
MI in plagioclase of Hek-16T
MI in olivine of HK2000T
Basalt
Basaltic andesite
Andesite
Dacite
Ryolite
Basalts of Vatnafjöll
Groundmass of HK2000T
SiO2 (wt%)
Na2O (wt%)
Al2O3 (wt%)
FeO* (wt%)
CaO (wt%)
TiO2 (wt%)
MgO (wt%)
P2O5 (wt%)
K2O (wt%)
a
b
c
d
e
f
g
h

Table 4
Standard reproducibility and estimated accuracy of major and volatile (Cl, S and F) elemental analysis

Samples	VG-A99 mean (±SD)	VG-A99 [a]	Ke12 mean (±SD)	Ke12 [b]
n	5 (major elements), 9 (S, Cl)		40 (major elements), 5 (Cl, F)	
SiO_2	50.7 (0.20)	50.9	69.4 (0.71)	70.0
TiO_2	4.13 (0.05)	4.06	0.27 (0.05)	0.28
Al_2O_3	12.1 (0.21)	12.5	7.66 (0.13)	7.73
FeO*	13.4 (0.13)	13.3	8.51 (0.17)	8.57
MnO	0.19 (0.01)	0.150	0.29 (0.04)	0.29
MgO	5.15 (0.02)	5.08	–	–
CaO	9.16 (0.07)	9.30	0.37 (0.03)	0.35
Na_2O	2.71 (0.13)	2.66	6.95 (0.14)	7.15
K_2O	0.862 (0.00)	0.820	4.39 (0.08)	4.14
P_2O_5	0.465 (0.02)	0.380	–	–
Sum	98.9 (0.17)	99.2	97.9 (0.81)	98.5
Cl	0.020 (0.001)	0.023 (0.002)	0.32 (0.01)	0.33 (0.01)
S	0.013 (0.001)	0.013 (0.005)	–	–
F	–	–	0.40 (0.02)	0.44 (0.11)

n = number of analyses.
Standard deviation is given in parenthesis.
–: Not determined.
[a] Recommended values for VG-A99 reference material for Cl and S concentrations [8,36]. Numbers in parenthesis represent the associated standard deviation.
[b] Recommended values for Ke12 reference material for chlorine [35] and for fluorine [37].

southern Iceland. Olivines hosting melt inclusions exhibit a compositional range from Fo71 to Fo84 ($n=8$; Table 1), whereas plagioclase phenocrysts enclosing MIs have a uniform composition (An66, $n=3$; Table 1). In contrast, the seven olivine phenocrysts containing MIs in the HK2000T basaltic icelandite have a constant forsterite content of 58% (Table 2). Melt inclusions in other minerals such as plagioclase (HK2000T), augite or titanomagnetite were either partially crystallized or absent. Detailed search by scanning electron microscope (SEM) and backscattering secondary electron imaging for sulphide globules or minerals in both samples was unsuccessful.

5.2. MIs — compositional variability

5.2.1. MIs in basalt

The corrected compositions of MIs in phenocrysts from the Hek-16T basalt show significant variation with, for instance, MgO ranging from 4.60 to 7.73 wt.% (Table 1). This variation is reflected in the composition of the host olivine: the highest Fo-content corresponds to melt inclusions with lowest K_2O concentration (0.47± 0.10 wt.%; Fig. 3). Furthermore, the MIs A and 2A, which are hosted by the same olivine phenocryst (Fo78), exhibit very similar major and volatile element composition (Table 1). These evidences strongly imply that the MIs were trapped in olivine phenocrysts growing from an evolving basaltic magma and consequently represent the liquid-line-of-descent for the parental basaltic magma of Hekla volcanic system. The most evolved olivine-hosted MI (GL in Table 1; $K_2O=0.64$ wt.%) is indistinguishable from plagioclase-hosted MIs in terms of its major and volatile element composition (Table 1, Fig. 2). The GL-inclusion also has the largest observed bubble, 6% by volume (Table 1) and therefore has the highest potential for being affected by post-entrapment volatile diffusion into bubble [42,43].

Concentrations of Cl, S, F and H_2O in olivine MIs are in the range of 124–264 ppm, 1444–2626 ppm, 229–672 ppm and 5600–7100 ppm, respectively, whereas those in plagioclase MIs range from 202 to 248 ppm Cl, from 2056 to 2584 ppm S and from 426 to 628 ppm F. Furthermore, in these basalt MIs the volatile element concentrations evolve in a similar manner as K_2O: the highest volatile element concentrations are observed in the most evolved MIs hosted by the low-Fo olivines and the plagioclases phenocrysts (Table 1, Fig. 4).

5.2.2. MI and groundmass in basaltic icelandite

The analyses of major and volatile elements in the melt inclusions of the HK2000T basaltic icelandite, as well as those of the whole rock and the groundmass, are listed in Table 2. The MI-bearing olivine phenocrysts in the basaltic icelandite have homogeneous Fo-content (Fo58) and their MIs exhibit consequently a uniform major and

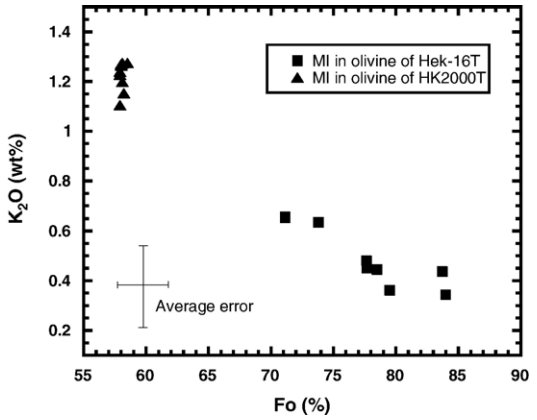

Fig. 3. Correlation between the composition of the host olivine (Fo%) and K_2O of the corresponding MIs in the 1913 Hekla basalt and the 2000 basaltic icelandite. Average 2σ error is plotted.

volatile element compositions (Fig. 3). With the exception of the HK2000T groundmass glass, these MI-compositions are the most evolved ones observed in this study (K_2O=1.19±0.05 wt.%; Table 2). Furthermore, their composition is very similar to the whole rock sample (Table 2). Therefore, we conclude that these MIs are representative of the basaltic icelandite magma of the 2000 eruption as well as the magma erupted during the final phase of historic Hekla eruptions (Fig. 2). Clearly, this does not hold for Na concentrations because our Na-analyses are underestimated in the HK2000T MIs.

As expected in closed-system behaviour, volatiles are more concentrated in MIs from the most evolved basaltic icelandite, with the notable exception of sulphur (see below). In the HK2000T MIs the volatile concentrations range from 379 to 421 ppm for Cl, from 978 to 1393 ppm for F and from 918 to 993 ppm in S. An analysis from a one MI gave 2.42±0.34 wt.% for H_2O. In addition, we observe no significant difference in S, Cl and F concentrations between MIs containing or not containing a shrinkage bubble, implying that the concentration of these elements has not been modified by post-entrapment diffusion into shrinkage bubbles (Table 2).

Five spot-analyses performed on the HK2000T groundmass glass yield a mean concentration of 374±28 ppm for Cl (range: 340–410 ppm), 1117±17 ppm for F (1100–1146 ppm) and 268±41 ppm for S (219–310 ppm). The groundmass glass appears to contain negligible water based on the LOI measurement of the bulk sample (Table 2). After applying our correction for the effects of microlite crystallisation in the groundmass, the volatile element and potassium concentrations are: 282±21 ppm Cl, 843±13 ppm F, 203±31 ppm S and 1.16±0.08 wt.% K_2O (Table 2). These values are comparable to the concentrations previously measured in the 1970 basaltic icelandite of Hekla, using different analytical techniques [44,45].

Taken as a whole, the melt compositions recorded by the MIs reflect the magma evolution from the most primitive basaltic lavas encountered around Hekla towards the least evolved magma erupted by Hekla volcano *sensu stricto* [18].

6. Discussion

6.1. Do the MIs represent magma at depth?

Although major element compositions of the MIs fall on the evolutionary trend of Hekla lavas (Fig. 2), it remains to demonstrate whether their volatile concentrations represent those of the undegassed magma at depth. Inclusions may leak if fractures are present (e.g. [43]), hydrogen may diffuse out of the inclusion and fast-diffusing species may enter from the melt around the host crystals into the MIs (e.g. [46,47]). Moreover, MIs may form in minerals crystallising from partially degassed magma. In this study, only MIs with no visible fracture or dislocation boundaries were chosen for analyses.

The MIs in Hekla's basalt can be assumed to be undegassed for S, Cl, F and H_2O based on the following arguments. Their Cl/K_2O is close to the value of 0.04, typical for the Iceland plume ([48] and references therein), and a specific signature compared to other oceanic intraplate basalts [49]. Moreover, their H_2O, F, Cl concentrations and S/Cl are close to those from other mantle-plume related magmas ([50–54]; Fig. 5). In addition, their water concentrations and H_2O/K_2O are also consistent with those measured in subglacial basaltic glasses from Iceland, which are likely to reflect juvenile water concentrations [55].

No direct arguments can be used to assess if the volatile concentrations in MIs in the basaltic icelandite represent those of the undegassed magma, but several indirect lines of evidences are presented below.

6.1.1. Comparison with other EVZ basalts

The compositions of basalts in Iceland are thought to represent different mixtures of mantle melts from the Iceland plume and the depleted upper mantle reservoir from which mid-ocean ridge basalts (MORB) are derived (e.g. [56,57]). Three types of basalts occur in the Eastern Volcanic Zone: tholeiites in the northern part, transitional alkaline basalts (or FeTi-rich basalts) in the central part and alkaline basalt farthest to the south (e.g. [24]). Volatile measurements in MIs from tholeiites of Laki and Veidivötn volcanic systems [13,58,59] show

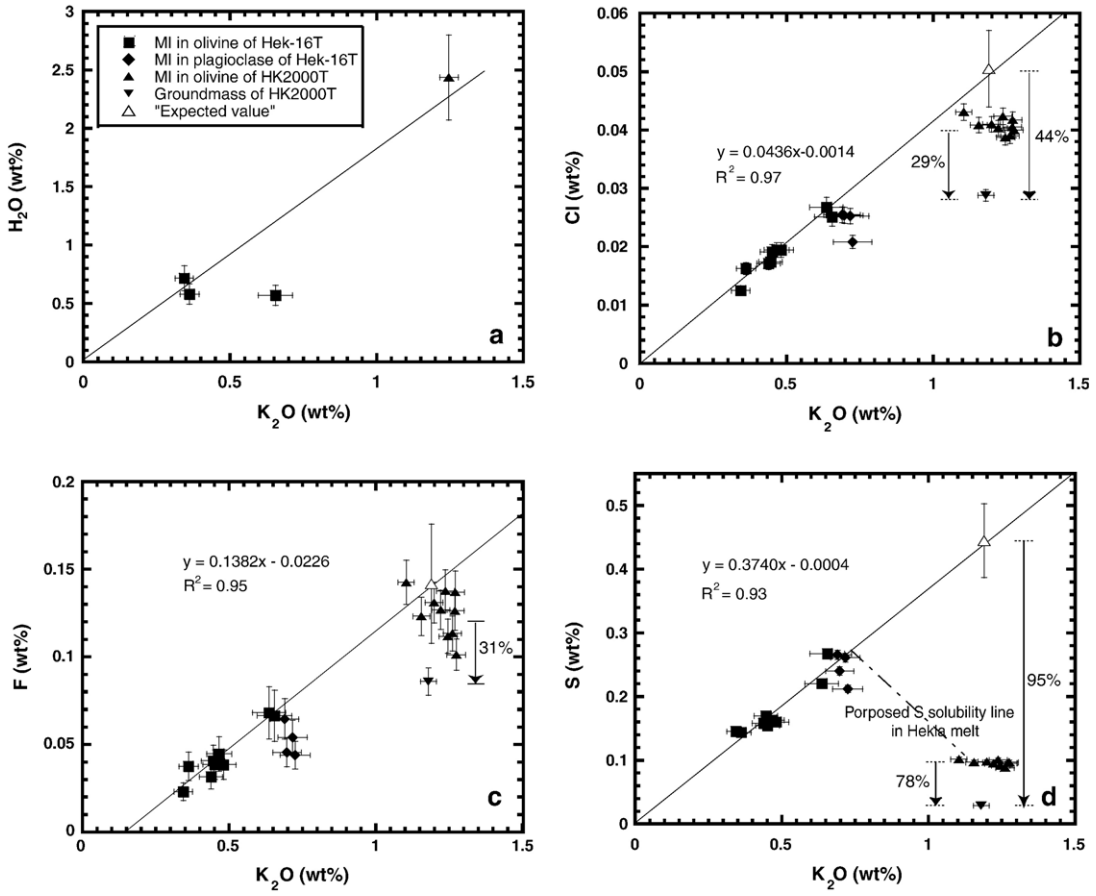

Fig. 4. Evolution of the dissolved volatile concentrations in Hekla magmas. The corrected F, S, Cl and K_2O values of the basaltic icelandite groundmass are plotted. For water, a line passing through origin and the two basaltic MIs extrapolates through the single analysed MI of the basaltic icelandite. Calculated York-type regression lines through the MIs trapped in 1913 basalt olivines, thought to be undegassed, are displayed for Cl, F and S in Fig. 4b, c and d. In Fig. 4c, the calculated regression line does not pass through the origin but given the overall uncertainties on the F concentrations, a straight line is readily drawn from the origin and through the inclusion data of both the basalt and the basaltic icelandite. The "expected" concentrations of volatile elements in basaltic icelandite magmas before eruption are calculated from the extrapolation of this line to the average K_2O value of the basaltic icelandite MIs. The estimated degree of degassing (in %) during the 2000 eruption is also shown. Minimum degree of degassing is calculated from the difference of the measured concentrations in the inclusions of the HK2000T and the groundmass value, whereas the maximum value is calculated from the expected value and the groundmass value. Also shown (dashed line) is the proposed S solubility line for the differentiation process between the most evolved basaltic MIs and those in basaltic icelandite due to titanomagnetite crystallisation (decrease in Fe concentration in melt and therefore S solubility; see text for further discussions). Error bars (2σ) for the "expected values" are calculated from the error on the regression line (see the algorithm of calculation of York [82]).

greater variations in their S/Cl values than MIs from the basalt of Hekla and Katla (Fig. 5). Notably, the latter plot close to the proposed hot spot values of Métrich et al. ([54]; Fig. 5), whereas MIs from the tholeiites form a linear array between the presumed hot spot and MORB values. These results suggest that the hot spot signature is less diluted in the off-rift transitional alkaline basalts, such as at Hekla and Katla, than in the rift-related tholeiites. Taken together, the coherence between tectonic setting and the volatile compositions of the MI basalt compositions in the EVZ strongly suggests that the MIs of the different basalts either have all degassed in a similar manner or, much more likely, represent the composition of undegassed primitive melts at depth.

6.1.2. Volatile saturation in basaltic MIs

The composition of MIs in the Hekla basalt matches not only the known compositional range for volatiles but also that of the major elements in MIs of other EVZ basalts. Sulphur and total iron, expressed as FeO*, concentrations in the EVZ inclusions are positively correlated (for Hekla $R^2=0.7$; Fig. 6), illustrating the well-known relationship between sulphur solubility and iron concentration in basaltic magmas [60,61]. However, sulphur solubility depends on several parameters,

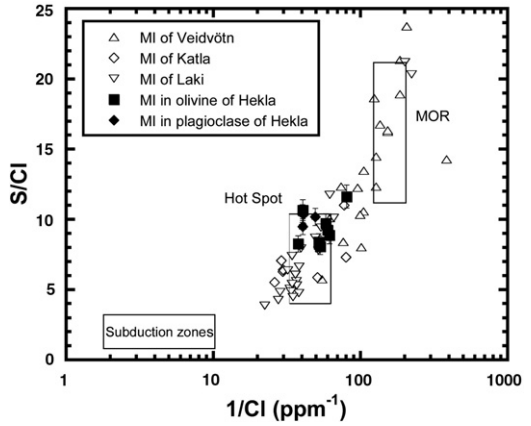

Fig. 5. The S/Cl values versus 1/Cl for melt inclusions of Hekla basalts compared to those from the EVZ of Iceland [8,13,58,59]. The three boxes outline the proposed compositional fields for MIs from volcanoes of subduction zones, hot spots and mid-ocean ridges (MOR) [54]. MIs from Hekla and Katla plot in or close to the Hot Spot field, whereas those from Veidivötn and Laki fall on a trend linking the MOR and the Hot Spot fields. Note that the MIs from Laki with the highest S/Cl are exclusively observed in glasses with MgO > 8%.

such as pressure, temperature, fO_2, fS_2, and bulk composition, particularly FeO content of magmas (e.g. [32,62–65]). The exact saturation curve for sulphur in basalts is unknown but the Hekla results show a trend of higher sulphur concentration at given FeO*, compared to mid-ocean ridge basalts [61,66]. This discrepancy most likely reflects relatively higher oxygen fugacity in Hekla magmas compared to that of MORB but it may also be partly attributed to differences in magma temperatures and bulk compositions [61]. However, sulphur measurements from other EVZ basalt MIs fall on an array slightly below the saturation limit of MORBs [13]. In this context, it is worth noting that oxygen fugacity in Icelandic magmas has not yet been thoroughly investigated.

Moreover, the basaltic magma of Hekla appears to be undersaturated in water since the predicted water concentration of basalts, assuming CO_2 between 0 and 2 wt.% at pressure close to 0.3 GPa [67], ranges between 3.5 and 5 wt.%, compared to the measured 0.6 wt.% in the MIs of the Hek-16T basalt. This pressure corresponds to the estimated 9 km depth of Hekla's magma chamber [25]. Furthermore, the saturation levels for Cl and F in basalts are poorly constrained but the comparison between magma compositions at Hekla and experimental results for basalts and andesites [62,68] suggests that Cl and F are well below the saturation level in basaltic magmas from the Hekla system. Hence it is reasonable to assume that volatiles other than S and CO_2 are undersaturated in the MIs of Hekla basalt. The absence of hydrous minerals and apatite in our samples lends support to this assumption. Consequently, the evolution of these volatiles will be strongly controlled by crystal-liquid differentiation processes [69].

6.2. Volatile evolution during basalt-basaltic icelandite fractional crystallisation

The main process forming the basaltic icelandites of Hekla is fractional crystallisation of basaltic magma similar that erupted in the vicinity of Hekla, as verified by systematic variations of major and trace elements and both stable and radiogenic isotope ratios [18]. The crystallising assemblage is olivine, plagioclase, clinopyroxene and titanomagnetite. The fact that the MI compositions match the evolutionary trend defined by whole compositions confirms that fractional crystallisation alone can account for the liquid-line-of-descent from the less evolved inclusions to the most evolved groundmass of the basaltic icelandite (Fig. 2). Such a simple differentiation mechanism allows us to predict and evaluate the behaviour of the volatile elements in Hekla magmas prior to entrapment in the phenocrysts of the basaltic icelandite. Earlier studies have clearly shown how the incompatible behaviour of volatile elements during fractional crystallisation can be used to track magma evolution and degassing [4,5,11].

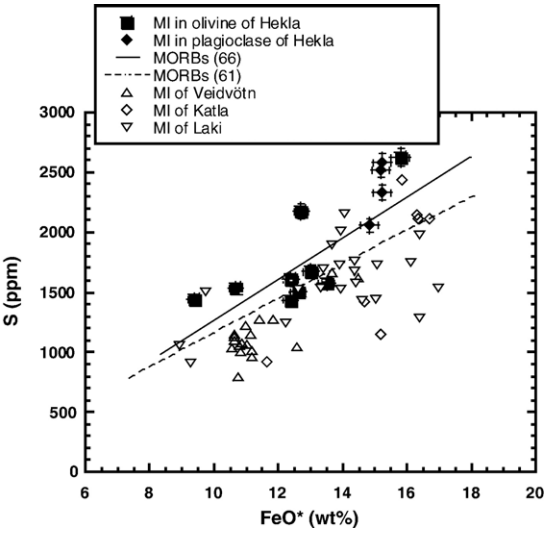

Fig. 6. Sulphur concentration as a function of FeO* in melt inclusions of Hekla basalts compared to those of other EVZ volcanoes [8,13,58] and to glass of submarine lava flows from mid-oceanic ridges [61,66]. Error bars (2σ) are shown for the MIs of Hekla. Higher S concentrations at a given FeO* in the Hekla MIs suggest that sulphur solubility is higher at Hekla compared to what has been proposed for MORB.

6.2.1. Degree of crystal fractionation

Fig. 2 shows the variation of major elements as a function of K_2O, which is a good index of magma differentiation at Hekla. Comparison between potassium and thorium concentrations in whole rocks for the entire Hekla magma suite [18] reveals that the bulk partition coefficient of K_2O between crystals and liquid (D_{K_2O}) is close to 0.2 for the relevant interval of magma differentiation. This value is obtained from the slope of a linear correlation ($R^2=0.99$) on a logK_2O–logTh plot assuming negligible D_{Th}, which is justified by the absence of accessory minerals in the Hekla products. This D_{K_2O} agrees with published values (e.g. [70]). From the Raleigh-fractionation law, the change in K_2O from the most primitive (MI in basalt) to the most evolved melt (basaltic icelandite matrix composition corrected for the presence of microlite) can be accounted for by 83% crystal fractionation. In other words, the groundmass of the basaltic icelandite, prior to microlite crystallization, corresponds to a remaining melt fraction of 17%.

6.2.2. Volatile evolution during fractional crystallization

The evolution of the volatile concentrations during fractional crystallisation from the most primitive inclusions towards those of the basaltic icelandite is displayed in Fig. 4. Water, Cl and F in the MIs increase systematically with K_2O, whereas S concentration increases steadily with K_2O in MIs of the basalt and then drop to the lowest measured values in MIs of the basaltic icelandite. In all instances, the groundmass value falls below the linear arrays in Fig. 4. In terms of water contents (Fig. 4a), the most evolved MI of the basalt (GL) has the lowest H_2O value, most likely because of water diffusion into the shrinkage bubble after entrapment (see above). However, the only MI in the basaltic icelandite analysed for water has no bubble (Table 2) and its water content correlates with the two pristine MIs of the basalt and extrapolates through the origin.

Best regression line was calculated through the olivine MI results for Cl, F and S from the basalt since these MIs are inferred to be undegassed and record the more primitive part of the liquid-line-of-decent. The linear correlations from all three diagrams pass close to the origin (Fig. 4). In detail, however, extrapolation of the Cl–K_2O correlation towards the K_2O of the basaltic icelandite yield slightly but significantly higher Cl than measured in the MIs (Fig. 4b). Assuming a similar behaviour of Cl and K_2O during crystal fractionation, this value is the one that would be "expected" in the absence of any Cl degassing. A somewhat different behaviour is found for fluorine versus potassium, whose correlation line extrapolates through the highest F values in the MIs of the basaltic icelandite (Fig. 4c). The best fit through the sulphur variations also extrapolates through the origin, but the significantly lower S concentrations of MIs in the basaltic icelandite clearly show that S has been separated from the evolving melt (Fig. 4d). From the linear correlations in Fig. 4, the bulk partition coefficients between crystals and the basaltic melt for the volatile elements can be estimated as: $D_{Cl} \approx D_S \approx D_{K_2O} \geq D_F$, illustrating the incompatible behaviour of volatile elements in the Hekla magma. The "expected" initial volatile concentrations in the basaltic icelandite MIs for Cl and F are 505±65 ppm and 1417±340 ppm, respectively (see Fig. 4), whereas that for S is as high as 4447±530 ppm (Fig. 4d). Such a high S concentration is well beyond the estimated S solubility in basaltic icelandite and thus cannot have been totally dissolved in the basaltic icelandite melt of Hekla. It is likely that significant amount of S was stored in a sulphur-rich exsolved fluid or melt phase in the Hekla magma chamber (see below).

6.2.3. Comparison of expected and measured volatile concentrations

Although water is the dominant volatile species in silicate melts, no loss of this volatile is observed in the single MI in the basaltic icelandite analysed with SIMS ($H_2O=2.42$ wt.%; Fig. 4a). Saturation of F was not reached in the magma and no evidence is found for F depletion in the MIs. In contrast, even if saturation may not have been attained for chlorine, this volatile appears to be slightly degassed from the MIs of the basaltic icelandite (Fig. 4b) presumably due to extensive CO_2 degassing. On the other hand, significant amount of S is missing. This degassing pattern suggests a similar and higher solubility of H_2O and F in Hekla magma than for Cl and S-species, in agreement with theoretical considerations [62] and degassing model [71].

6.3. Causes of sulphur loss before entrapment of MIs in basaltic icelandite

The relatively low S concentrations measured in the MIs of the basaltic icelandite reveal that, before the formation of the inclusions, significant amount of S had been removed from the melt. Since the oxygen fugacity in the Hekla magma is close to FMQ [15], the sulphur occurs mainly as sulphide [10,33]. Therefore, either partial sulphide degassing, immiscibility and/or crystallisation could have lowered the sulphur concentration in the melt prior to MI entrapment. The absence of sulphide minerals and globules in our samples suggests that either these high-density

phases were gravitationally separated from the evolving silicate melt [72] or that sulphur was partially removed as H_2S in a vapour phase. Early degassing of CO_2 could indeed have helped carry H_2S towards the magma chamber roof [73], contributing to the explosive sup-Plinian phase.

In any case, a significant change in sulphur solubility is likely to have occurred before MIs entrapment in basaltic icelandite. The solubility is likely to decrease with diminishing Fe concentrations as a result of crystallisation of titanomagnetite (Fig. 2e,f). Fractionation of FeTi-oxides is directly reflected in the concentration variations of Ti that reach a maximum at 0.7 wt.% K_2O, at the onset of titanomagnetite fractionation. The regular decrease in TiO_2 and FeO with further differentiation as measured in the Hekla lavas is likely to mimic that of S as well, and therefore its solubility (Fig. 4d). To a first approximation, the decreasing concentrations of both FeO* and TiO_2 from the evolved basalt to the basaltic icelandite follow a near-linear trend. We assume that S concentrations will follow a similar path and decrease linearly (Fig. 4d). Therefore, the maximum amount of S that may have been degassed during the 2000 eruption of Hekla can be estimated from the difference between the "expected" S value and the measured concentration of the degassed groundmass glass (see Fig. 4d). A minimum amount is given by the difference between the MIs and the groundmass of the basaltic icelandite itself, i.e. using the "petrological method".

6.4. Estimation of volatile release during the 2000 Hekla eruption

The differences in volatile contents between MIs in basaltic icelandites and groundmass corrected for the degree of crystallisation, indicate a minimum degassing of about 29% Cl, 78% S and 31% F (Fig. 4; Table 5), which are similar to the values calculated for the Laki eruption [8]. Differences between the "expected" values for MIs in basaltic icelandite (Fig. 4) and those of the groundmass yield upper limits of ~44% Cl, 95% S and 31% F. The water content of the groundmass glass was not measured and therefore the water degassing is not discussed here. The volatile mass released during the 2000 Hekla eruption can then be estimated: Taking 0.17 km^3 for the total volume of erupted magma [26] and a density of 2610 $kg \cdot m^{-3}$ for a basaltic icelandite melt, one obtains 0.05–0.1 Mt of HCl, 0.6–3.8 Mt of SO_2 and 0.17 Mt of HF (Table 5). Our lower estimate for sulphur outgassing is close to that given by Sharma et al. [12]. Since non-erupted magma may contribute to the volatile mass balance, "petrological" estimates can only be conservative [6,8]. Non-erupted magma can potentially be a mass of degassed magma that was left at depth at the end of the eruption due to faster ascent of the gas phase relative to the magmatic liquid.

6.4.1. Comparison of estimated magma degassing and the measured composition of the 2000 Plinian gas phase

During the February–March 2000 eruption of Hekla, snowstorms fell through the eruption column condensing and scavenging the gas phase, which was sampled as snow (e.g. [22]). These snow samples thus provide a proxy to determine the composition and the volatile ratios of the gas phase during the early sub-Plinian phase of the eruption. The F/Cl in the different snow samples range from 0.7 (±0.03) to 2.2 (±0.09; [22]), whereas those estimated from the differences between MI of the basaltic icelandite and the groundmass glass composition is 3.3 (±0.44) and those defined by the differences between "expected" concentrations and matrix glass composition is 1.7 (±0.31). Such a reasonably good similarity of F/Cl in snow samples and in MI-based estimates justifies the approach used in this study.

Sulphur in the snow samples was principally condensed as SO_4^{2-} [74]. This condensate represents only a part of the total emitted sulphur released in less oxidized forms such as H_2S, S_2 or SO_2. Therefore, sulphur degassing estimated from the composition of the MIs cannot be compared with the snow samples. However, satellite-based spectroscopic measurements during the eruption detected the emission of 0.13–0.37 Mt of SO_2, and up to 0.008 Mt of sulphate [28]. These results are lower than ours by factor of 2 to 10, but this can be explained by intrinsic limitations in the satellite-based sensing techniques used to infer Hekla's sulphur emissions (TOMS — Total Ozone Mapping Spectrometer-and MODIS — Moderate Resolution Imaging Spectroradiameter-[29]). TOMS estimates are affected by the high-latitude location of Hekla combined with the low solar energy during polar winter, as stated by Rose et al. [28]. Similarly, the MODIS values are underestimates owing to cold underlying temperatures, and the presence of ice in the plume that strongly affects IR spectra [28]. Furthermore, during the initial sub-Plinian phase (26 February), when most of the eruptive gases were emitted [25,26], significantly lower values were measured due to "very high optical depth of the volcanic plume" [28]. Nevertheless, we emphasize that the remote sensing values for the Hekla eruption are comparable to the lower sulphur degassing estimates from this study and that of Sharma et al. [12]. We thus can conclude that all these studies [12,28, this study] provide a fairly good estimate of the quantity of sulphur released during the effusive phase of the Hekla 2000 eruption.

Table 5
Estimates of the mass (in Mt) of volatiles dissolved in the Hekla magma prior to the 2000 eruption, and released during the eruption and the degree of magma degassing (in %)

	SO_2	HCl	HF
Minimum and maximum mass in 2000 Hekla magma (mr)	0.825 (±0.024)–3.95 (±0.12)	0.180 (±0.005)–0.231 (±0.03)	0.565 (±0.124)
Minimum and maximum mass released during the 2000 eruption (mb)	0.645 (±0.026)–3.77 (±0.16)	0.052 (±0.002)–0.102 (±0.013)	0.172 (±0.022)
Minimum and maxium degree (%) of degassing	78–95	29–44	31

$mr = V_r \rho \varepsilon \upsilon_{x,ic}$ or $mr = V_r \rho \varepsilon \upsilon_{x,i}$ where V_r is the total volume of magma erupted, ρ is the basaltic icelandite magma density: 2610 kg m^{-3}, ε is the factor required to convert pure element to element compounds, $\upsilon_{x,ic}$ is the maximum concentration expected of element x in melt inclusions in basaltic icelandite (0.44 wt.% for S, 0.05 wt.% for Cl and 0.12 wt.% for F) and $\upsilon_{x,i}$ is the measured concentration of element x in MIs of the basaltic icelandite (note that when taking into account the 2σ errors on the "expected" values, $\upsilon_{x,i}$ becomes equal to $\upsilon_{x,ic}$ for fluorine).
$mb = V_r \rho \varepsilon (\upsilon_{x,i} - \upsilon_{x,gc})$ or $mb = V_r \rho \varepsilon (\upsilon_{x,ic} - \upsilon_{x,gc})$ where $\upsilon_{x,gc}$ is the corrected concentration of element x in the groundmass glass of the basaltic icelandite.

The improved approach presented here and the reducing conditions of the Hekla magmas indicate that much sulphur could be either exsolved in a sulphide vapour phase (as H_2S or even S_2) and/or accumulated in a reducing immiscible sulphide liquid segregated from its silicic host during the magma differentiation and prior to MI entrapment. The latter explanation appears less likely since no traces of sulphide minerals or globules are observed in Hekla lavas. However, it cannot be eliminated but all sulphur trapped by such a hypothetical immiscible sulphide liquid is likely to volatilize upon eruption [75]. The preferred explanation for the difference between the remote sensing values (0.13–0.37 Mt of SO_2) and our higher estimate (3.8 Mt of sulphur calculated as SO_2) appears to be the early formation of a sulphide vapour phase [e.g. 69,76] promoted by early exsolution of CO_2 (and CO [14], as observed at surface and illustrates the reducing conditions at depth) in the magma column. Gas accumulation beneath the roof of the magma chamber prior to the 2000 eruption of Hekla and its sudden release during the initial sub-Plinian eruption are compatible with the estimated high magma velocity (9 km in 1/2 h, or 5 m/s; [77]). Sulphur species in the gas phase are principally sulphur dioxide (SO_2) and hydrogen sulphide (H_2S) but S_2 and H_2SO_4 would also be present [78]. The relative proportions of the two main species in the volatile phase are principally controlled by temperature, pressure and oxygen fugacity in the melt (e.g. [62]). H_2S is favoured in reduced melt, and despite the probable oxidation of H_2S during atmospheric transport (e.g. [69]), the H_2S/SO_2 at equilibrium can be as high as 3 [79]. Due to the low oxygen fugacity of Hekla and other hot spot related magmas, reduced sulphur species (H_2S and S_2) were likely present in its gas plume. This could explain the difference between our approach in estimating sulphur degassing and that of the remote sensing methods [28] which are unable to detect H_2S and other reduced sulphur species. In addition, a part of the sulphur emitted during the eruption could have been rapidly adsorbed on tephra grains and/or trapped in ice crystals, which formed in the volcanic plume [74,80]. Such a phenomenon was observed during the 1970 Hekla eruption whose tephra showed widespread adsorption of sulphate and H_2SO_4 [81]. In summary, we conclude that the total amount of sulphur that was degassed during the 2000 Hekla eruption may easily be an order of magnitude greater than previously estimated from remote sensing techniques.

7. Conclusions

The simple magma differentiation, fractional crystallisation, recorded by the composition of melt inclusions in basalt and in basaltic icelandite of Hekla volcano permits us to trace the evolution of dissolved volatiles in its magmatic system. The compositions of MIs in these two rock types reflect the magma evolution from the most primitive lavas encountered around Hekla towards the least evolved magma erupted by Hekla itself. The co-variations of volatile concentrations with K_2O yield the estimated concentrations in the basaltic icelandite melt just prior to eruption. Using this approach, we observe that water and fluorine had not been exsolved from the magma at the time of MI-formation, whereas chlorine and especially sulphur were degassed before the melt entrapment. This approach thus avoids underestimation of pre-eruptive volatile contents and leads to improved estimates of the volatile mass release into the atmosphere. Finally, this method also yields better constraints on the "excess S" postulate, for instance.

Acknowledgements

We thank P. Allard and P.J. Wallace for constructive reviews that led to significant improvements of the manuscript. We are most grateful to Gudrun Larsen for supplying the tephra sample from the 2000 Hekla eruption. Jean-Luc Devidal and François Faure are acknowledged for their help with the analytical work and Regis Doucelance for discussion on error analyses. We thank the Smithsonian National Museum of Natural History's assistance and Nicole Métrich for providing VG-A99 and Ke12 standard glasses, respectively. A grant from the "Jules Verne" programme of the French–Icelandic scientific collaboration partially financed the fieldwork. The French INSU-CNRS programme PNRN grant covered the analytical cost.

References

[1] M.R. Rampino, S. Self, Volcanic winter and accelerated glaciation following the Toba super-eruption, Nature 359 (1992) 50–52.
[2] T. Thordarson, D.J. Miller, G. Larsen, S. Self, H. Sigurdsson, New estimates of sulfur degassing and atmospheric mass-loading by the 934 AD Eldjà eruption, Iceland, J. Volcanol. Geotherm. Res. 108 (2001) 33–54.
[3] A. Robock, Introduction: Mount Pinatubo as a test of climate feedback mechanisms, in: A. Robock, C. Oppenheimer (Eds.), Volcanism and the Earth's Atmosphere, Geophysical Monograph, Washington DC, 2003, pp. 1–8.
[4] A.T. Anderson, Chlorine, sulfur, and water in magmas and oceans, Geol. Soc. Amer. Bull. 85 (1974) 1485–1492.
[5] P.J. Wallace, From mantle to atmosphere: magma degassing, explosive eruptions, and volcanic volatile budgets, in: B. De Vivo, R.J. Bodnar (Eds.), Melt Inclusions in Volcanic Systems. Methods, Applications and Problems, Elsevier Sciences B.V., Amsterdam, 2003, pp. 105–127.
[6] J.D. Devine, H. Sigurdsson, A.N. Davis, S. Self, Estimates of sulfur and chlorine yield to the atmosphere from volcanic eruptions and potential climatic effects, J. Geophys. Res. 89 (1984) 6309–6325.
[7] J.M. Palais, H. Sigurdsson, Petrologic evidence of volatile emissions from major historic and pre-historic volcanic eruptions, in: M.W. Kidson (Ed.), Understanding Climate Change. American Geophysical Union, Geophys. Monograph., 1989, pp. 31–53.
[8] T. Thordarson, S. Self, N. Oskarsson, T. Hulsebosh, Sulfur, chlorine and fluorine degassing and atmospheric loading by the 1783–1784 AD Laki (Skaftar Fires) eruption in Iceland, Bull. Volcanol. 58 (1996) 205–225.
[9] T.V. Gerlach, H.R. Westrich, T.J. Casadevall, D.L. Finnegan, Vapor saturation and accumulation in magmas of the 1989–1990 eruption of Redoubt volcano, Alaska, J. Volcanol. Geotherm. Res. 62 (1994) 317–337.
[10] B. Scaillet, J.F. Luhr, M.R. Carroll, Petrological and volcanological constraints on volcanic sulfur emissions to the atmosphere, in: A. Robock, C. Oppenheimer (Eds.), Volcanism and the Earth's atmosphere, Geophysical Monograph, Washington DC, 2003, pp. 11–40.
[11] M. Edmonds, D.M. Pyle, C. Oppenheimer, A model for degassing at the Soufriere Hills Volcano, Montserrat, West Indies, based on geochemical data, Earth Planet. Sci. Lett. 186 (2001) 159–173.
[12] K. Sharma, S. Blake, S. Self, A.J. Krueger, SO_2 emissions from basaltic eruptions, and the excess sulfur issue, Geophys. Res. Lett. 31 (2004), doi:10.1029/2004GL019688.
[13] T. Thordarson, S. Self, J.M. Miller, G. Larsen, E.G. Vilmundardottir, Sulphur release from flood lava eruptions in the Veidivötn, Grimsvötn and Katla volcanic sytems, Iceland, in: C. Oppenheimer, D.M. Pyle, J. Barclay (Eds.), Volcanic Degassing, Geological Society, London, 2003, pp. 103–121.
[14] S. Thorarinsson, The eruption of Hekla 1947–48. 1—the eruptions of Hekla in historical times, a tephrochronological study, Soc. Sci. Isl. (1967) 1–170.
[15] W.S. Baldridge, T.R. McGetchin, F.A. Frey, Magmatic evolution of Hekla, Iceland, Contrib. Mineral. Petrol. 42 (1973) 245–258.
[16] G.E. Sigvaldason, The petrology of Hekla and origin of silicic rocks in Iceland, eruption of Hekla 1947–48, Soc. Sci. Isl. 5 (1974) 1–44.
[17] A. Gudmundsson, N. Oskarsson, K. Gronvold, K. Saemundsson, O. Sigurdsson, R. Stefansson, S.R. Gislason, P. Einarsson, B. Brandsdottir, G. Larsen, H. Johannesson, T. Thordarson, The 1991 eruption of Hekla, Iceland, Bull. Volcanol. 54 (1992) 238–246.
[18] O. Sigmarsson, M. Condomines, S. Fourcade, A detailed Th, Sr and O isotope study of Hekla: differentiation processes in an Icelandic volcano, Contrib. Mineral. Petrol. 112 (1992) 20–34.
[19] N. Oskarsson, The interaction between volcanic gases and tephra: fluorine adhering to tephra of the 1970 Hekla eruption, J. Volcanol. Geotherm. Res. 8 (1980) 251–266.
[20] N. Oskarsson, The chemistry of Icelandic lava incrustations and the latest stages of degassing, J. Volcanol. Geotherm. Res. 10 (1981) 93–111.
[21] P. Frogner, S.R. Gislason, N. Oskarsson, Fertilizing potential of volcanic ash in ocean surface water, Geology 29 (2001) 473–568.
[22] S. Moune, P.J. Gauthier, S.R. Gislason, O. Sigmarsson, Trace element degassing and enrichment in the eruptive plume of the 2000 eruption of Hekla volcano, Iceland, Geochim. Cosmochim. Acta 70 (2006) 461–479.
[23] T. Thordarson, G. Larsen, Volcanism in Iceland in historical time: volcano types, eruption styles and eruptive history, J. Geodyn. (2006), doi:10.1016/j.jog.2006.09.005.
[24] S.P. Jakobsson, Petrology of recent basalts from the eastern volcanic zone, Iceland, Acta Nat. Isl. 26 (1979) 1–103.
[25] E. Sturkell, K. Agustsson, A.T. Linde, S.I. Sacks, P. Einarsson, F. Sigmundsson, H. Geirsson, R. Pedersen, Geodetic constraints on the magma chamber of the Hekla volcano, Iceland, AGU, San Francisco, 2005.
[26] C. Lacasse, S. Karlsdottir, G. Larsen, H. Soosalu, W.I. Rose, G.G.J. Ernst, Weather radar observations of the Hekla 2000 eruption cloud, Iceland, Bull. Volcanol. 66 (2004) 457–473.
[27] K.O. Haraldsson, S.G. Arnason, G. Larsen, J. Eiriksson, The Hekla eruption of 2000 — the tephra fall, Proceedings of the 25th Nordic Geological Winter Meeting, Abstracts volume, Reykjavik, 2002, p. 71.
[28] W.I. Rose, Y. Gu, I.M. Watson, T. Yu, G.J.S. Bluth, A.J. Prata, A.J. Krueger, N. Krotkov, S. Carn, M.D. Fromm, D.E. Hunton, G.G.J. Ernst, A.A. Viggiano, J.M. Miller, J.O. Ballenthin, J.M. Reeves, J.C. Wilson, B.E. Anderson, D.E. Flittner, The February–March 2000 eruption of Hekla, Iceland from a satellite perspective, in: A.

Robock, C. Oppenheimer (Eds.), Geophys. Monograph, Amer. Geophys. Union, Washington DC, 2003, pp. 107–132.
[29] D.E. Hunton, A.A. Viggiano, J.M. Miller, J.O. Ballenthin, J.M. Reeves, J.C. Wilson, S.H. Lee, B.E. Anderson, W.H. Brune, H. Harder, J.B. Simpas, N. Oskarsson, In-situ aircraft observations of the 2000 Mt. Hekla volcanic cloud: compositions and chemical evolution in the Arctic lower stratosphere, J. Volcanol. Geotherm. Res. 145 (2005) 23–34.
[30] J.B. Lowenstern, Melt inclusions come of age: volatiles, volcanoes, and Sorby's legacy, in: B.D.V.a.R.J. Bodnar (Ed.), Melt Inclusions in Volcanic Systems: Methods, Applications and Problems, Elsevier Press, Amsterdam, 2003, pp. 1–22.
[31] J.B. Hunt, P.G. Hill, Tephrological implications of beam size-sample-size effects in electron microprobe analysis of glass shards, J. Quat. Sci. 16 (2001) 105–117.
[32] P.J. Wallace, I.S.E. Carmichael, S speciation in submarine basaltic glasses as determined by measurements of SKa X-ray wavelength shifts, Am. Mineral. 79 (1994) 161–167.
[33] N. Métrich, R. Clochhiatti, Sulfur abundance and its speciation in oxidized alkaline melts, Geochim. Cosmochim. Acta 60 (1996) 4151–4160.
[34] M. Ancey, F. Bastenaire, R. Tixier, Applications des méthodes statistiques en microanalyse, in: F. Maurice, L. Meny, R. Tixier (Eds.), Microanalyse microscopie électronique à balayage, Les éditions de physique, Les Ulis, vol. 7, 1978, pp. 323–339.
[35] N. Métrich, M.J. Rutherford, Experimental study of chlorine behaviour in hydrous silicic melts, Geochim. Cosmochim. Acta 56 (1991) 606–616.
[36] E. Jarosewich, J.A. Nelen, J.A. Norberg, Electron microprobe reference samples for mineral analysis, Smithson, Contrib. Earth Sci. 22 (1979).
[37] J.B. Witter, S.M. Kuehner, A simple empirical method for high-quality electron microprobe analysis of fluorine at trace levels in Fe-bearing minerals and glasses, Am. Mineral. 89 (2004) 57–63.
[38] E. Deloule, O. Paillat, M. Pichavant, B. Scaillet, Ion microprobe determination of water in silicate glasses: methods and applications, Chem. Geol. 125 (1995) 19–28.
[39] P.L. Roedder, R.F. Emslie, Olivine-liquid equilibrium, Contrib. Mineral. Petrol. 29 (1970) 275–289.
[40] M.J. Toplis, The thermodynamics of iron and magnesium partitioning between olivine and liquid: criteria for assessing and predicting equilibrium in natural and experimental systems, Contrib. Mineral. Petrol. 149 (2005) 22–39.
[41] A. Kilinc, I.S.E. Carmichael, M.L. Rivers, R.O. Sack, The ferric–ferrous ratio of natural silicate liquids equilibrated in air, Contrib. Mineral. Petrol. 83 (1983) 136–140.
[42] A.T. Anderson, S. Newman, S.N. Williams, T.H. Druitt, C. Skirius, E. Stolper, H_2O, CO_2, Cl, and gas in Plinian and ash-flow Bishop rhyolite, Geology 17 (1989) 221–225.
[43] J.B. Lowenstern, Applications of silicate-melt inclusions to the study of magmatic volatiles, in: J.H.F.E. Thompson (Ed.), Magmas, Fluid and Ore deposits, Mineralogist Association of Canada short course, British Columbia, Victoria, 1995, pp. 71–99.
[44] G.E. Sigvaldason, N. Oskarsson, Chlorine in basalts from Iceland, Geochim. Cosmochim. Acta 40 (1976) 777–789.
[45] G.E. Sigvaldason, N. Oskarsson, Fluorine in basalts from Iceland, Contrib. Mineral. Petrol 94 (1986) 236–271.
[46] D. Massare, N. Métrich, R. Clocchiatti, High-temperature experiments on silicate melt inclusions in olivine at 1 atm: inference on temperatures of homogenization and H_2O concentrations, Chem. Geol. 183 (2002) 87–98.
[47] E. Cottrell, M. Spiegelmann, C.H. Langmuir, Consequences of diffusive reequilibration for the interpretation of melt inclusions, Geochem. Geophys. Geosyst. 3 (2002), doi:10.1029/2001GC000205.
[48] A. Jambon, B. Déruelle, G. Dreibus, F. Pineau, Chlorine and bromine abundance in MORB: the contrasting behaviour of the Mid-Atlantic Ridge and East Pacific Rise and implications for chlorine geodynamic cycle, Chem. Geol. 126 (1995) 101–117.
[49] N.A. Stroncik, K.M. Haase, Chlorine in oceanic intraplate basalts: constraints on mantle sources and recycling processes, Geology 32 (2004) 945–948.
[50] J.G. Schilling, M.B. Bergeron, R. Evans, Halogens in the mantle beneath the North Atlantic, Philos. Trans. R. Soc. Lond., A 297 (1980) 147–178.
[51] H. Bureau, Les éléments volatils associés aux magmas du Piton de la Fournaise : une approche par l'étude des inclusions fluides et vitreuses, PhD Thesis, Paris 7 Denis Diderot, 1996.
[52] J.E. Dixon, D.A. Clague, Volatiles in basaltic glasses from Loihi Seamount, Hawaii: evidence for a relatively dry plume component, J. Petrol. 42 (2001) 627–654.
[53] J.C. Lassiter, E. Hauri, I.K. Nikogosian, H.G. Barsczus, Chlorine-potassium variations in melt inclusions from Raivavae and Rapa, Austral Islands: constraints on chlorine recycling in the mantle and evidence for brine-induced melting of oceanic crust, Earth Planet. Sci. Lett. 202 (2002) 525–540.
[54] N. Métrich, P. Allard, N. Spilliaert, D. Andronico, M. Burton, 2001 flank eruption of the alkali-and volatile-rich primitive basalt responsible for Mount Etna's evolution in the last three decades, Earth Planet. Sci. Lett. 228 (2004) 1–17.
[55] A.R.L. Nichols, M.R. Carroll, A. Hoskuldsson, Is the Iceland hot spot also wet? Evidence from the water contents of undegassed submarine and subglacial pillow basalts, Earth Planet. Sci. Lett. 202 (2002) 77–87.
[56] J.G. Schilling, Iceland mantle plume: geochemical study of reykjanes ridge, Nature 242 (1973) 565–571.
[57] O. Sigmarsson, S. Steinthorsson, Origin of Icelandic basalts: a review of their petrology and geochemistry, J. Geodyn. (2006), doi:10.1016/j.jog.2006.09.016.
[58] N. Métrich, H. Sigurdsson, P.S. Meyer, J.D. Devine, The 1783 Lakagigar eruption in Iceland: geochemistry, CO_2 and sulfur degassing, Contrib. Mineral. Petrol. 107 (1991) 435–447.
[59] T. Thordarson, Volatile release and atmospheric effects of basaltic fissure eruptions, PhD Thesis, University of Hawaii, 1995.
[60] D.R. Haughton, P.L. Roeder, B.J. Skinner, Solubility of sulfur in mafic magmas, Econ. Geol. 69 (1974) 451–467.
[61] P.J. Wallace, I.S.E. Carmichael, Sulfur in basaltic magmas, Geochim. Cosmochim. Acta 65 (1992) 1863–1874.
[62] M.R. Carroll, J.D. Webster, Solubilities of sulfur, noble gases, nitrogen, chlorine, and fluorine in magmas, in: M.R. Carroll, J.R. Holloway (Eds.), Volatiles in Magmas, Mineralogical Society of America, Washington DC, 1994, pp. 231–271.
[63] R.F. Wendlandt, Sulfide saturation of basalt and andesite melts at high pressures and temperatures, Am. Mineral. 67 (1982) 877–885.
[64] J.A. Mavrogenes, H.S.C. O'Neill, The relative effects of pressure, temperature and oxygen fugacity on the solubility of sulfide in mafic magmas, Geochim. Cosmochim. Acta 63 (1999) 1173–1180.
[65] P.J. Jugo, R.W. Luth, J.P. Richards, Experimental data on the speciation of sulfur as a function of oxygen fugacity in basaltic melts, Geochim. Cosmochim. Acta 69 (2005) 497–503.

[66] E.A. Mathez, Sulfur solubility and magmatic sulfides in submarine glass, J. Geophys. Res. 81 (1976) 4269–4276.
[67] P. Papale, Modelling of the solubility of a one component H_2O or CO_2 fluid in silicate liquids, Contrib. Mineral. Petrol. 126 (1997) 237–251.
[68] J.D. Webster, R.J. Kinzler, E.A. Mathez, Chloride and water solubility in basalt and andesite melts and implications for magmatic degassing, Geochim. Cosmochim. Acta 63 (1999) 729–738.
[69] P.J. Wallace, Volcanic SO_2 emissions and the abundance and distribution of exsolved gas in magma bodies, J. Volcanol. Geotherm. Res. 108 (2001) 85–106.
[70] J.A. Philpotts, C.C. Schnetzler, Phenocryst-matrix partition coefficients for K, Rb, Sr and Ba, with applications to anorthosite and basalt genesis, Geochim. Cosmochim. Acta 34 (1970) 307–322.
[71] A. Aiuppa, C. Federico, A. Paonita, G. Pecoraino, M. Valenza, S, Cl and F degassing as an indicator of volcanic dynamics: the 2001 eruption of Mount Etna, Geophys. Res. Lett. 29 (2002), doi:10.1029/2002GL015032.
[72] V.C. Kress, Thermochemistry of sulfide liquids. I. The system O–S–Fe at 1 bar, Contrib. Mineral. Petrol. 127 (1997) 176–186.
[73] C. Jaupart, S. Vergniolle, The generation and collapse of a loam layer at the roof of a basaltic magma chamber, J. Fluid Mech. 203 (1989) 347–380.
[74] C. Textor, H.F. Graf, M. Herzog, Injection of gases into the stratosphere by explosive volcanic eruptions, J. Geophys. Res. 108-D19 (ACH 5) (2003) 1–17, doi:10.1029/2002JD002987.
[75] T.M. Gerlach, H.R. Westrich, R.B. Symonds, Pre-eruption vapor in magma of the climactic Mount Pinatubo eruption: source of the giant stratospheric sulfur dioxide cloud, in: C.G. Newhall, R.S. Punongbayan (Eds.), Fire and Mud: Eruptions and Lahars of Mount Pinatubo, Philippines, University of Washington Press, Seattle WA, 1996, pp. 415–433.
[76] B. Scaillet, B. Clemente, B.W. Evans, M. Pichavant, Redox control of sulfur degassing in silicic magmas, J. Geophys. Res. 103 (1998) 23,937–23,949.
[77] H. Soosalu, P. Einarsson, Seismic constraints on magma chambers at Hekla and Torfajökull volcanoes, Iceland, Bull. Volcanol. 66 (2004) 276–286.
[78] T.S. Bates, B.K. Lamb, A. Guenther, J. Dignon, R.E. Stoiber, Sulfur emissions to the atmosphere from natural sources, J. Atmos. Chem. 14 (1992) 315–337.
[79] R.B. Symonds, W.I. Rose, G.J.S. Bluth, T.M. Gerlach, Volcanic gas studies: methods, results and applications, in: M.R. Carroll, J.R. Holloway (Eds.), Volatiles in Magmas, Mineralogical Society of America, Washington DC, 1994, pp. 1–66.
[80] W.I. Rose, Scavenging of volcanic aerosol by ash: atmospheric and volcanologic implications, Geology 5 (1977) 621–624.
[81] R.D. Cadle, I.H. Blifford, Hekla eruption clouds, Nature 230 (1971) 573–574.
[82] D. York, Least squares fitting of a straight line with correlated errors, Earth Planet. Sci. Lett. 5 (1969) 320–324.